

ARTICLE

Open Access

# Closed-crown packaging system for stable, long-term neural recording in group-housed mice

Yeonghwa Hong<sup>1</sup>, Giheon Kim<sup>2</sup>, Haeyun Lee<sup>2</sup>, Hyeonggyeong Cha<sup>1</sup>, Minseok Kim<sup>2</sup>, Se Hwan Park<sup>2</sup>, Seungjun Lee<sup>2,3</sup>, Namsun Chou<sup>3,4</sup>✉ and Hyogeun Shin<sup>1,2,5</sup>✉

## Abstract

Long-term recording of neural circuit activity in behaving mice is essential for understanding the pathophysiology of neuropsychiatric disorders and developing effective therapies. However, conventional open-crown packaging leaves cables and connectors exposed, making them vulnerable to biting, mechanical impact, and contamination. In group-housing conditions, these weaknesses often cause cable disconnection or probe damage, forcing single housing and undermining the ecological validity of studies on social behavior. To address these limitations, we developed a closed-crown neural probe packaging system that (i) integrates an NFC-enabled crown for simultaneous physical shielding and individual identification, (ii) employs an ultra-thin PSR-based flexible cable (~35 μm) to ensure mechanical flexibility and stable long-term connectivity, and (iii) incorporates black Pt–electroplated electrodes with low impedance (the tens of kilohms at 1 kHz) for stable neural recording. After implantation into the hippocampal CA1 region, mice maintained under group-housing conditions exhibited stable impedance over extended periods, with preserved spike waveform and signal-to-noise ratio. Behavioral assessments showed no signs of packaging-induced social stress, and anxiety-related indices were improved in group-housed mice compared with isolated ones. In summary, the proposed closed-crown system provides a robust platform for stable, long-term neural recording under naturalistic social conditions. This approach enables precise examination of neural circuit dynamics in socially interacting animals and offers a powerful tool for advancing the study of social behavior and neuropsychiatric disorders.

## Introduction

Mice are among the most widely used animal models in neuroscience research because of their genetic similarity to humans<sup>1–3</sup> and their complex social behaviors<sup>4–8</sup>. In particular, studies combining neural signal analysis with electrical stimulation have been instrumental in elucidating the pathophysiology of psychiatric disorders such as depression and anxiety, as well as in developing novel therapeutic strategies<sup>9–12</sup>. To enable such investigations with greater precision and systematic control, an array of advanced neuroscientific tools has been developed,

including neural probes for recording electrical activity<sup>13–16</sup>, optogenetic systems for targeted control of gene expression<sup>17–19</sup>, and optical imaging platforms for monitoring calcium dynamics<sup>20–22</sup>. Together, these technologies have made it possible to analyze neural activity in real time within behaving animals<sup>23–26</sup>.

Among these approaches, neural probes are especially valuable because they provide precise recordings of electrical activity at the cellular level, offering critical insights into the functional organization of neural circuits in the brain<sup>27,28</sup>. Recent studies increasingly emphasize the need to examine neural activity during natural, unrestrained behaviors, underscoring the importance of implantable electrodes and robust packaging technologies that support stable, long-term recordings under socially relevant housing conditions<sup>29,30</sup>.

Traditionally, packaging systems are implemented to protect neural probes implanted in the brain, typically

Correspondence: Namsun Chou (nschou@kbri.re.kr) or Hyogeun Shin (hyogeunshin@knu.ac.kr)

<sup>1</sup>School of Electronics Engineering, Kyungpook National University, Daegu, Republic of Korea

<sup>2</sup>School of Electronic and Electrical Engineering, Kyungpook National University, Daegu, Republic of Korea

Full list of author information is available at the end of the article

© The Author(s) 2026



**Open Access** This article is licensed under a Creative Commons Attribution-NonCommercial-NoDerivatives 4.0 International License, which permits any non-commercial use, sharing, distribution and reproduction in any medium or format, as long as you give appropriate credit to the original author(s) and the source, provide a link to the Creative Commons licence, and indicate if you modified the licensed material. You do not have permission under this licence to share adapted material derived from this article or parts of it. The images or other third party material in this article are included in the article's Creative Commons licence, unless indicated otherwise in a credit line to the material. If material is not included in the article's Creative Commons licence and your intended use is not permitted by statutory regulation or exceeds the permitted use, you will need to obtain permission directly from the copyright holder. To view a copy of this licence, visit <http://creativecommons.org/licenses/by-nc-nd/4.0/>.

using open-crown head-mount designs<sup>23,24,31–33</sup> or fully encapsulating structures based on dental cement<sup>34–39</sup>. In this configuration, the connector and connecting cables remain exposed, leaving them vulnerable to biting, pulling, or disconnection caused by interactions among animals in group housing (Fig. S1). Consequently, many experiments require animals with implants to be housed individually. Such isolation eliminates social interaction and is well known to induce a range of physiological and behavioral abnormalities, including increased anxiety, depressive-like behaviors, and reduced locomotor activity, thereby potentially confounding both behavioral readouts and neural recordings and compromising the reliability and ecological validity of neural data<sup>40–45</sup>.

To address these limitations, we developed a closed-crown neural probe packaging system designed for long-term, stable neural recordings under group-housing conditions (Fig. 1). The closed-crown design provides comprehensive protection for probes and cables, effectively preventing damage from environmental exposure or animal interaction (Fig. 1a). The system also integrates a near-field communication (NFC) tag within the crown for efficient individual identification and employs a highly flexible photo solder resist (PSR)-based cable to accommodate natural movement, enabling stable neural recording during behavioral experiments (Fig. 1b).

We validated the performance of this system by maintaining mice implanted with the closed-crown assembly under group-housing conditions for over a month while continuously recording neural signals. The system demonstrated stable impedance and preserved spike signal quality over multiple weeks, without mechanical failures. Furthermore, behavioral assays revealed that isolated mice displayed elevated anxiety and altered social interaction patterns with group-housed counterparts, whereas group housing preserved normal behavioral profiles regardless of crown implantation.

Overall, the proposed closed-crown packaging system enables reliable long-term neural recording under group-housing conditions. This system provides a novel and powerful research platform for investigating how social environments shape neural circuit dynamics and behavior, offering valuable opportunities for advancing the study of social isolation-related neuropsychiatric disorders and other socially influenced brain functions.

## Materials and Methods

### Fabrication and characterization of neural probe system

To enable long-term neural signal recording in group-housed mice, we fabricated a silicon-based neural probe following established microfabrication protocols<sup>46,47</sup>. The probe featured a shank 100  $\mu\text{m}$  wide, 15  $\mu\text{m}$  thick, and 6 mm long, with eight recording electrodes linearly arranged along the shank. Each electrode measured 20  $\times$

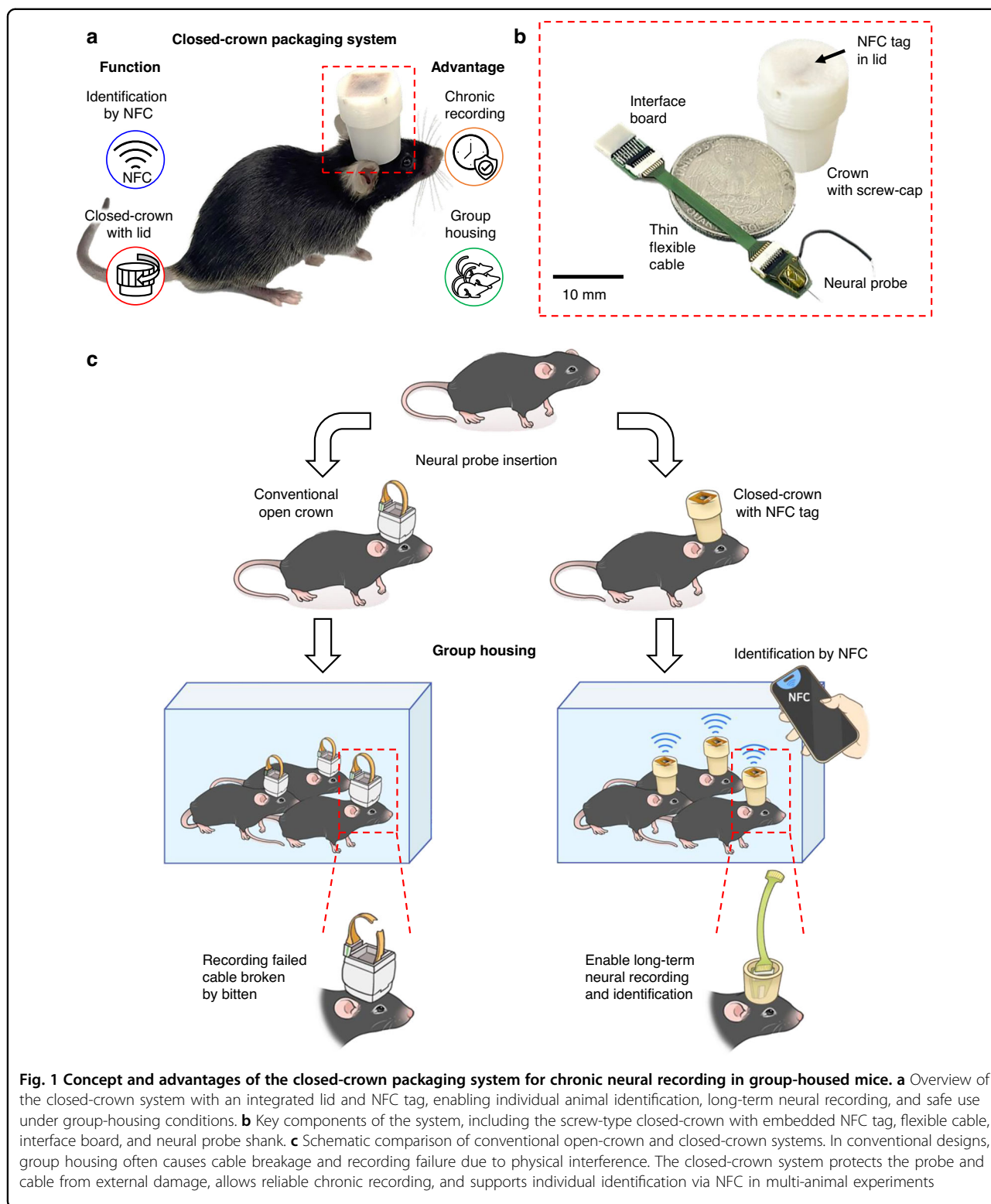
20  $\mu\text{m}$ , with a center-to-center spacing of 40  $\mu\text{m}$ . For signal interfacing, a custom printed circuit board (PCB) measuring 7.25 mm  $\times$  9.7 mm was designed and fabricated, and connected to a flexible printed circuit (FPC) connector (5034801000, Molex, USA).

To improve electrochemical performance, a black platinum (black Pt) layer was electrodeposited on the platinum electrode sites by applying a constant current of  $-1 \mu\text{A}$  for 60 s per electrode (PalmSens 4, PalmSens B.V., Netherlands)<sup>47</sup>. To compare the surface roughness of the electroplated black Pt electrodes with that of conventional Pt electrodes, surface morphology was characterized using an atomic force microscope (AFM; NX20, Park Systems, Republic of Korea). AFM imaging was performed over an area of  $2.5 \times 2.5 \mu\text{m}^2$  at a scan rate of 0.5 Hz. Electrochemical impedance spectroscopy (EIS) was performed in  $1\times$  phosphate-buffered saline (PBS, room temperature) to evaluate impedance characteristics before and after coating. Cyclic voltammetry (CV) was conducted over a potential range of  $-0.5 \text{ V}$  to  $0.8 \text{ V}$  at a scan rate of 50 mV/s to assess the electrochemical reactivity of both conventional Pt and black Pt electrodes. Electrode durability was further verified by repeating CV measurements 60 consecutive times under identical conditions.

To enhance flexibility and mechanical resilience during movement, we replaced the conventional polyimide (PI)-based cable (thickness = 120  $\mu\text{m}$ ) with an ultrathin PSR-based flexible cable (thickness = 35  $\mu\text{m}$ ) developed in our previous studies<sup>48,49</sup>. The mechanical stability of the PSR-based cable was assessed by twisting the cable while monitoring resistance changes using a probe station (MST-5500, MS TECH, Republic of Korea).

To evaluate the durability of the cables under repetitive bending, a syringe pump (NE-4000, New Era Syringe Pump Inc., USA) was used as a linear actuator to perform cyclic bending tests. The samples were repeatedly bent from an initial gap of 2 cm to a bending radius of  $r = 2 \text{ mm}$ . Electrical resistance was measured using a probe station, and resistance variation and deviation were quantitatively compared between PI and PSR cables as a function of bending cycles.

In addition, to characterize the bending compliance of the PSR-based cable, the bending reaction force was measured using a custom-built sensing module incorporating a force-sensitive resistor (FSR402, Interlink Electronics, USA). The sensing module consisted of a compliant foam layer to evenly distribute the applied force across the FSR surface, a rigid pad to transmit the force, and a glass backing plate to provide mechanical support. The glass plate was fixed using a 3D-printed fixture. Two identical sensing modules were positioned facing each other, and the reaction force was recorded while incrementally increasing the number of cable turns. The FSR output signals were conditioned through a custom



interface board for sensitivity optimization and acquired using a microcontroller unit (Arduino Uno, Arduino, Italy). The measured force values were calibrated to Newton units using a 50 g reference weight.

Finally, to protect the wire bonds between the PCB and the probe and to mechanically secure the flexible cable, a thermosetting epoxy (OD2002, EPO-TEK, USA) was applied and cured on a hot plate at 100 °C for 40 minutes.

The probe, PSR-based flexible cable, and PCB were then integrated into a single, compact neural probe system suitable for long-term and stable recordings.

#### **Fabrication and characterization of closed-crown packaging system**

To stably support the neural probe system on the head and protect it from external environmental factors, a closed-crown structure was fabricated using a 3D printer (Creality K1 Max, Creality, China) with Hyper ABS filament (CREALITY, China). Depending on the experimental requirements, two crown designs were developed: a slide-lid type optimized for lightweight configuration and a screw-cap type designed to maximize mechanical stability.

The slide-lid crown featured a tapered cuboid geometry, with a top size of  $12 \times 13 \text{ mm}^2$ , a bottom size of  $9 \times 9 \text{ mm}^2$ , and a height of 18 mm. To further reduce weight, grid-like side windows were incorporated, and a small top handle was added to facilitate easy manipulation during installation or removal. In contrast, the screw-cap crown had a cylindrical geometry with a top diameter of 15.5 mm, a bottom diameter of 10.5 mm, and a height of 20 mm. The threaded cap mechanism allowed the lid to be securely opened and closed, offering greater protection against mechanical stress.

A commercial NFC tag (Ntag 213, 180 bytes,  $10 \times 10 \times 0.1 \text{ mm}$ , S-RFID, Republic of Korea) was attached to the inner surface of each crown lid, enabling individual animal identification without visual labeling. The total weight of the NFC-integrated crowns was 0.79 g for the slide-lid type and 0.99 g for the screw-cap type, both sufficiently light to avoid affecting normal behavior or locomotion.

After fabrication, the closed-crown was mounted over the implanted probe system on the animal's skull. Once sealed, the structure provided complete protection of internal electrodes and connections from physical impact, external interference, and environmental contamination, ensuring long-term stability and reliability during behavioral experiments in group-housing conditions.

Because the force required to open the crown lid and the opening duration differ depending on the lid type, these parameters were quantitatively compared using a custom sensing module identical to that used for the cable reaction force measurements described in Section 2.1. For this experiment, the sensing module was attached directly to the fingertip without a backing plate, enabling real-time measurement of the applied force and opening time during lid actuation.

#### **In vivo surgical procedure**

All animal experiments were conducted in accordance with the guidelines of the Institutional Animal Care and Use Committee (IACUC) of the Korean Brain Research Institute (KBRI) (Approval No. IACUC-25-00039-M1).

For long-term neural signal recording and impedance measurements, an RHD recording system (Intan Technologies, USA) was employed. To interface the headstage with the implanted probe, a custom-designed interface PCB was fabricated, incorporating an Omnetics connector (Omnetics Connector Corporation, USA) and an FPC connector compatible with the flexible probe cable. All experiments were performed using adult male C57BL/6J mice (8 weeks old).

Surgical procedures were conducted under isoflurane anesthesia using an inhalation system (Screw Filler Cagemount, Medical Supplies & Services, UK). Anesthesia was induced at 4% and maintained at 1.5–2% throughout the procedure. Mice were positioned in an automated stereotaxic frame (71000 Automated Stereotaxic Instrument, RWD Life Science, USA), and the scalp was incised to expose the skull. Target coordinates for probe implantation were determined based on the Paxinos and Franklin Mouse Brain Atlas<sup>50</sup>.

Five small holes were drilled using a precision micro-drill. Three holes were designated for anchor screws to secure the probe assembly, and a central hole was used for probe insertion. A reference electrode screw was placed in the contralateral cerebral cortex. The neural probe was implanted into the hippocampal CA1 region at the following stereotaxic coordinates: mediolateral (ML) – 1.5 mm, anteroposterior (AP) – 1.75 mm, and dorsoventral (DV) – 1.75 mm. The implanted probe was fixed to the skull with stainless steel screws and dental cement (Vertex Self Curing, Vertex Dental, Netherlands). The closed-crown structure was then mounted above the skull using the same dental cement to provide mechanical protection and environmental shielding.

After surgery, mice were housed individually for one week of postoperative recovery. Following recovery, animals were divided into experimental housing conditions. In the group-housing condition, five to six male C57BL/6J mice were kept together in a single cage under a 12:12 h light–dark cycle. In single-housing conditions, mice were housed individually under identical environmental conditions. All animals had ad libitum access to food and water throughout the experimental period.

#### **Evaluation of crown protection strategies under group-housing conditions**

To directly compare the mechanical stability and durability of different probe encapsulation strategies under group-housing conditions, three packaging configurations were evaluated: (i) a conventional open-crown design, (ii) an open-crown temporarily sealed with medical adhesive tape, and (iii) the proposed closed-crown system.

All mice were implanted with identical neural probes and cable assemblies. Following implantation, animals were individually housed for a 1-week recovery period to

allow wound healing and stabilization of the implant. After recovery, mice were transferred to group-housing conditions under identical cage environments for all experimental groups.

For the open-crown condition, the probe connector and flexible cable were left fully exposed, reflecting commonly used conventional packaging approaches. For the tape-sealed condition, the open-crown was covered immediately after surgery using standard medical adhesive tape (Biotex adhesive plaster, Seoil Chemical Co., Republic of Korea), mimicking a temporary protective method sometimes employed in practice. For the closed-crown condition, the probe, connector, and cable were fully enclosed within a rigid crown body and sealed using a screw-cap lid.

After the transition to group housing, animals were continuously monitored by video recording for approximately 7.5 h to capture early-stage social interactions and mechanically induced stress caused by group behavior. This observation period was specifically used to directly compare damage occurrence between the open-crown and closed-crown configurations. In addition, visual inspections were performed at 24 h and 48 h after group housing to further assess the structural integrity of the cable, connector, and encapsulation system.

Mechanical failure was defined as visible cable deformation, partial tearing, or complete cable breakage that rendered neural recording impossible.

#### **Open field test: locomotor activity and anxiety-related behavioral experiments**

To evaluate the effects of crown weight, anxiety levels, and locomotor activity in mice exposed to different housing conditions over an extended period, we conducted an open field test (OFT)<sup>51,52</sup>. The testing arena was constructed from opaque acrylic and measured 40 × 40 cm<sup>2</sup>. A virtual grid divided the arena into two regions: the central 25% area, defined as the *center zone*, and the surrounding area, defined as the *peripheral zone*.

Each mouse was placed individually in the arena and allowed to freely explore for 10 minutes. All sessions were recorded at 30 fps using a Logitech camera. Recorded videos were analyzed using IDTracker software to extract trajectory coordinates, which were subsequently processed in MATLAB (MathWorks, USA) to quantify the following behavioral parameters:

- Total distance traveled
- Distance traveled within the center zone
- Time spent in the center zone
- Number of line crossings

These parameters were used to assess anxiety-related behavior and spontaneous locomotor activity, enabling comparison between group-housed and single-housed mice.

#### **Histological verification of electrode placement**

To verify accurate implantation of the neural probe into the hippocampal CA1 region, postmortem histological analysis was performed. Upon completion of the recording experiments, mice were transcardially perfused with phosphate-buffered saline (PBS), followed by fixation with 4% paraformaldehyde (PFA; Sigma-Aldrich). The brains were carefully extracted, post-fixed in 4% PFA for 24 h at 4 °C, and subsequently cryoprotected by immersion in a 30% (w/v) sucrose solution in PBS at 4 °C until they sank. The brains were then embedded in optimal cutting temperature (OCT) compound (Thermo Fisher Scientific).

The frozen brain blocks were sectioned coronally at a thickness of 50 μm using a cryostat (CM1860, Leica Microsystems, Wetzlar, Germany).

To visualize the electrode insertion trajectory, the neural probe shank was coated with rhodamine B (Sigma-Aldrich) immediately prior to implantation. For nuclear counterstaining, brain sections were incubated with DAPI (1 μg mL<sup>-1</sup>; Sigma-Aldrich) for 15 min following standard immunohistochemical procedures.

Fluorescence images of rhodamine B and DAPI were acquired using a confocal microscope (STELLARIS 8, Leica Microsystems, Wetzlar, Germany). The rhodamine B signal enabled identification of the electrode track, while DAPI staining delineated hippocampal anatomical layers, confirming probe placement within the CA1 region. All confocal images were acquired with a 100 μm scale bar.

#### **Electrophysiological recording and signal analysis**

Neural activity was recorded using an Intan electrophysiology system comprising the RHS stim/recording controller and RHS 16-channel stim/recording headstage (Intan Technologies, USA). The system was connected to the probe electrodes through the custom interface PCB, enabling stable signal transmission. Spike signals were continuously recorded for at least 5 minutes per session. Signal recordings were conducted in awake animals, which were briefly transferred to an isolated chamber for signal acquisition. Signal recording and impedance measurements commenced immediately after probe implantation (day 0) to confirm successful electrode placement and functional signal acquisition. To evaluate long-term recording stability and reliability, recordings were repeated weekly in group-housed mice.

All electrophysiological data were processed using RHX data acquisition software (Intan Technologies). The raw neural signals were digitized at a sampling rate of 20 kS/s per channel and filtered using a 0.3–7.5 kHz band-pass filter to isolate spike activity. A 60 Hz notch filter was

applied to eliminate power-line interference, and the signals were converted using a 16-bit analog-to-digital converter (ADC) to ensure data capture. Motion artifacts could occur during abrupt movements, including wall collisions or vigorous body shaking; therefore, neural signal analyses were conducted using only artifact-free recording segments. For post-processing, a threshold-based spike sorting algorithm, previously validated in the literature, was employed to detect and classify single-unit activity<sup>46</sup>. We quantified the noise level by calculating the standard deviation of the recorded signals<sup>53</sup>. The signal-to-noise ratio (SNR) was calculated by dividing the average peak amplitude of the classified signal by three times the noise level<sup>54</sup>.

### Social interaction behavioral experiments

To assess the effects of different housing conditions—group housing versus single housing—on social behavior, we performed a social interaction test using an unfamiliar mouse<sup>55,56</sup>. This experiment was designed to evaluate how social context influences locomotor activity and social engagement over time.

The behavioral testing arena was constructed from opaque white acrylic and measured  $35 \times 25 \times 25 \text{ cm}^3$ . A transparent acrylic cage ( $10 \times 10 \times 24 \text{ cm}^3$ ) containing an unfamiliar male mouse was positioned against one side of the arena wall. The cage had vertical bars spaced 5 mm apart, allowing the test mouse to approach, sniff, and interact while preventing physical contact. A “gray-shaded zone” was defined as the 7.5 cm area surrounding the stimulus cage, within which social interaction was quantified.

Adult male C57BL/6J mice (8 weeks old) were used in all experiments. On day 7 after neural probe implantation (day 0), animals were randomly assigned to group-housing or single-housing conditions. After a 10-day adaptation period (days 7–17), mice underwent a 2-day habituation phase (days 17–18) in the empty testing arena for 10 minutes per day to minimize novelty-induced behavioral responses in subsequent sessions.

The social interaction test was conducted weekly. In each session, the test mouse freely explored the arena for 10 minutes in the presence of an unfamiliar conspecific. To prevent fatigue and habituation effects, a new, unfamiliar mouse was introduced every 30 minutes. All sessions were recorded at 30 frames per second using a Logitech camera.

Behavioral trajectories were tracked using IDTracker software, and positional coordinates were processed in MATLAB (MathWorks, USA) to compute the following parameters:

- Total distance traveled
- Distance traveled within the gray-shaded zone
- Time spent within the gray-shaded zone

In addition, social interaction time was manually scored by a blinded experimenter using Clipchamp video editing software (Microsoft, USA), defined as the total duration during which the two mice engaged in social behaviors such as sniffing or touching each other.

### Statistical analysis

All statistical analyses were performed using MATLAB (MathWorks, USA) and GraphPad Prism (GraphPad Software, USA). Data were analyzed based on independent samples, and the specific statistical methods applied to each dataset are described in the corresponding figure legends. Statistical significance was determined according to standard thresholds.

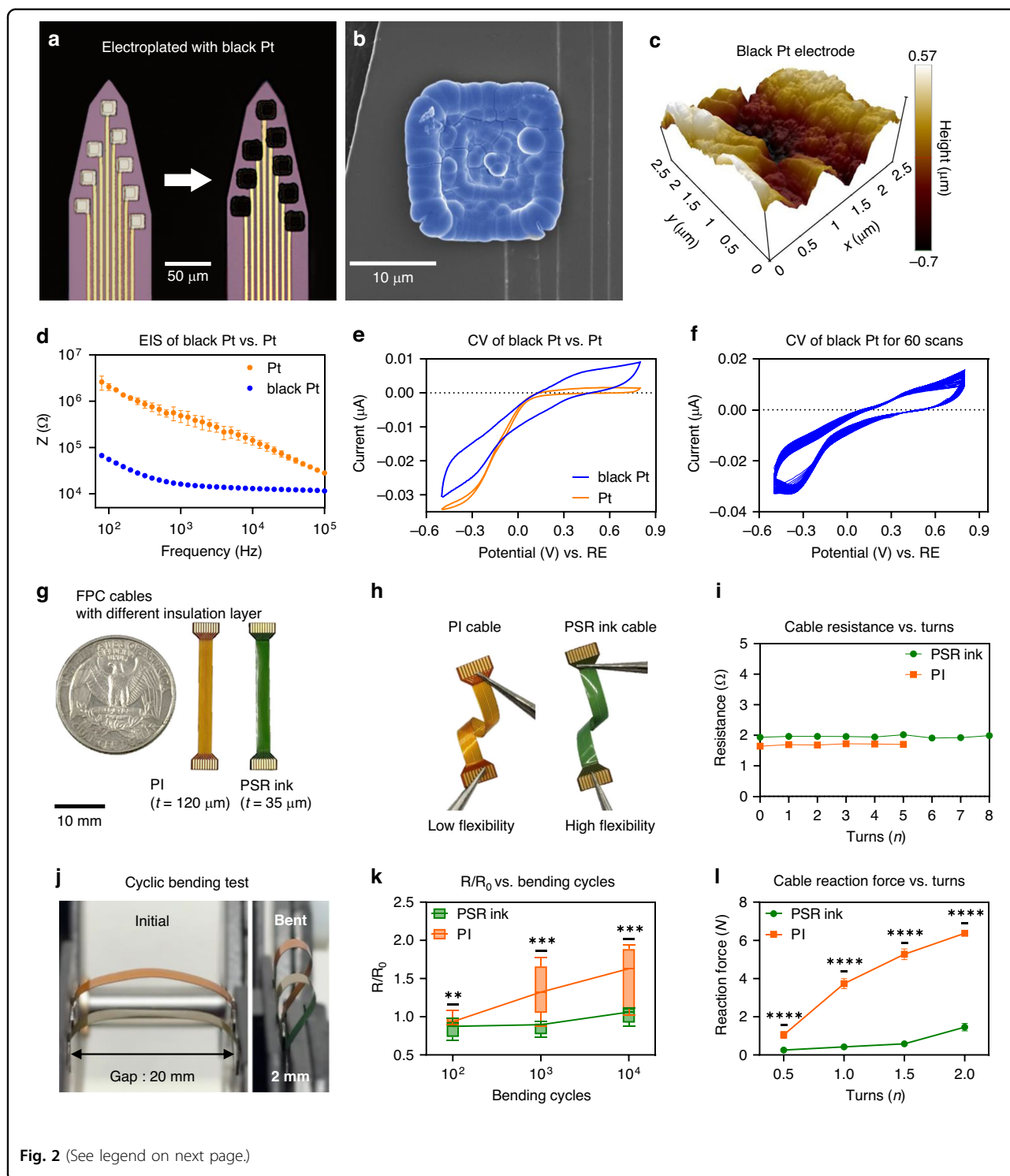
## Results and Discussion

### Concept of a closed-crown packaging system

Conventional neural probe packaging systems typically employ an open-crown design, leaving the connector and cable fully exposed to the external environment<sup>23,24,31–33</sup>. Under group-housing conditions, this exposed configuration frequently results in component damage or disconnection due to gnawing, pulling, or other physical interactions with cage mates (Figs. 1c,S1). Such failures often interrupt signal recording, prematurely terminate long-term experiments, and limit the feasibility of studies investigating social behaviors in mice.

To overcome these challenges, we developed a lightweight closed-crown packaging system that fully encloses the implanted probe and its connections, providing robust protection against external stimuli such as impact, biting, and scratching (Fig. 1). The structure functions as a protective cap, offering mechanical support and impact absorption, while reducing the risk of damage to both the connectors and cables. In addition, an NFC tag was integrated into the crown lid, enabling individual animal identification even in group-housed environments. This integration makes long-term neural recording and concurrent social behavior analysis feasible—capabilities that were difficult or impossible with conventional open-crown systems—while significantly enhancing system reliability.

Figure 1 illustrates the structural and functional differences between conventional open-crown and the newly developed closed-crown systems. Unlike traditional designs, in which connectors and cables are vulnerable to interactions with cage mates, the closed-crown system prevents physical damage and supports stable, long-term neural signal acquisition. Furthermore, the integrated NFC functionality facilitates automated individual identification, enabling simultaneous behavioral tracking and neural recording in socially housed animals, thereby bridging a critical gap in neuroscience research on naturalistic social behavior.



### Fabrication and characterization of neural probe and flexible cable

To demonstrate the general applicability of our approach, we employed a silicon-based neural probe widely used for neural signal recording. The probe was

fabricated using established microfabrication techniques<sup>46,47</sup>. The shank measured 100  $\mu\text{m}$  in width and 15  $\mu\text{m}$  in thickness and contained eight Pt recording electrodes (20  $\times$  20  $\mu\text{m}$  each) spaced 40  $\mu\text{m}$  center-to-center (Fig. 2a).

(see figure on previous page)

**Fig. 2 Electrochemical performance of black Pt electrodes and mechanical properties of ultrathin flexible cables.** **a** Optical images of electrode sites before and after black Pt electroplating. **b** SEM image showing the porous surface morphology of the black Pt coating. **c** Surface morphology characterization of the black Pt-coated electrode. **d** Electrochemical impedance spectroscopy (EIS) comparing conventional Pt and black Pt electrodes.  $n = 8$  (Electrode). **e** Cyclic voltammetry (CV) curves of Pt and black Pt electrodes. **f** CV stability test of black Pt electrodes over 60 consecutive scans. **g** Photographs of flexible printed circuit (FPC) cables fabricated with conventional polyimide (PI,  $t = 120 \mu\text{m}$ ) or photo solder resist (PSR,  $t = 35 \mu\text{m}$ ) insulation layers. **h** Comparison of mechanical flexibility between PI and PSR-based cables, highlighting enhanced flexibility with PSR insulation. **i** Cable resistance changes as a function of twisting turns, demonstrating mechanical durability and electrical stability. **j** Cyclic bending test setup for evaluating the mechanical durability of flexible cables. The cable was repeatedly bent with a fixed gap of 20 mm, and the minimum bending radius under deformation was approximately 2 mm. **k** Normalized electrical resistance change ( $R/R_0$ ) of PSR-based and PI-based cables as a function of bending cycles ( $10^2$ – $10^4$  cycles). Electrical resistance change:  $t(18) = 3.133$ ,  $p = 0.0057$  ( $10^2$  cycles);  $t(18) = 4.325$ ,  $p = 0.0004$  ( $10^3$  cycles);  $t(18) = 4.057$ ,  $p = 0.0007$  ( $10^4$  cycles). two-tailed unpaired  $t$ -test.  $**p < 0.01$ ,  $***p < 0.001$ .  $n = 10$  (samples). **l** Reaction force measured during cable twisting as a function of the number of turns. Reaction force:  $t(10) = 10.13$ ,  $p < 0.0001$  (0.5 turns);  $t(10) = 30.38$ ,  $p < 0.0001$  (1 turn);  $t(10) = 39.53$ ,  $p < 0.0001$  (1.5 turn);  $t(10) = 53.20$ ,  $p < 0.0001$  (2 turn). two-tailed unpaired  $t$ -test.  $****p < 0.0001$ .  $n = 6$  (samples). Data are presented as mean values  $\pm$  SD (**d**, **l**). Data are presented as mean values with minimum–maximum ranges (**k**)

To enhance electrochemical performance, the Pt electrodes were coated with black Pt via electrodeposition, creating a highly porous, rough surface that increased the effective surface area (Figs. 2b, c and S2). This modification significantly improved electrochemical reactivity and reduced electrode impedance (Fig. 2d–f). Electrochemical impedance spectroscopy (EIS) showed that black Pt electrodes exhibited 1–2 orders of magnitude lower impedance across the frequency range compared with conventional Pt electrodes (Fig. 2d). At 1 kHz—a critical frequency for neural recording—impedance decreased from  $485.1 \pm 140 \text{ k}\Omega$  (Pt) to  $16.1 \pm 0.3 \text{ k}\Omega$  (black Pt), well below the typical 5 M $\Omega$  threshold required for reliable signal detection (Fig. 2d)<sup>57</sup>. Cyclic voltammetry (CV) further demonstrated a marked increase in redox current, with stable performance maintained after 60 repeated scans, confirming excellent long-term electrochemical stability (Fig. 2e, f). These results quantitatively validate the suitability of black Pt-modified electrodes for chronic neural recordings.

To enable cable folding within the closed-crown structure, we optimized the flexible interconnect cable. Using a photo-solder resist (PSR)-based layer instead of conventional polyimide (PI), the cable thickness was reduced to  $\sim 35 \mu\text{m}$ —significantly thinner than standard PI cables ( $\sim 120 \mu\text{m}$ ) (Fig. 2g)<sup>48,49</sup>. This design enhanced flexibility, reduced crown height, minimized movement constraints, and decreased mechanical stress transmitted to the probe, thereby reducing the risk of displacement in the brain. Beyond single-probe applications, the ultrathin PSR-based cable is compatible with multi-shank neural probes, facilitating scalability for high-throughput recordings. The closed-crown packaging structure accommodates multiple shanks without mechanical interference, supporting integration of increased electrode counts while preserving probe stability.

Mechanical testing revealed that PSR-based cables could withstand up to eight twists, compared with five for conventional cables, while maintaining stable electrical

resistance even after repeated bending (Fig. 2h, i and Movie S1). Also, the mechanical durability of the flexible cables under repetitive deformation was evaluated using cyclic bending tests (Fig. 2j) and Movie S2). The PSR-based cable maintained a nearly constant normalized resistance even after  $10^4$  bending cycles, whereas the conventional PI cable exhibited a clear, cycle-dependent increase in resistance, indicating progressive mechanical fatigue (Fig. 2k). This contrast demonstrates that the PSR-based cable possesses superior resistance to repeated bending while preserving electrical stability. To further evaluate mechanical compliance, the bending reaction force was independently quantified (Fig. S3). As the number of cable turns increased, the PSR-based cable consistently generated significantly lower reaction forces than the PI cable, reflecting its reduced stiffness and enhanced flexibility (Fig. 2l). The lower mechanical loading imposed by the PSR cable suggests minimized stress transmission to the neural probe and connector during cable–probe interconnection, thereby reducing the risk of mechanical fatigue and probe displacement. These results demonstrate both high mechanical durability and electrical stability.

In summary, the integration of black Pt electrodes and an ultrathin PSR-based flexible cable produced a neural probe system with excellent electrochemical performance, mechanical flexibility, and signal stability.

### Design and assembly of closed-crown packaging with NFC integration

Unlike conventional open-crown systems, which primarily provide basic protection for implanted neural probes, we developed a closed-crown packaging structure capable of robustly shielding the entire probe system, even under group-housing conditions (Fig. S4). The core design objectives were four aspects:

- (i) Complete structural protection of the probe and cable against mechanical impact and environmental disturbances.

- (ii) A lid structure that allows reliable signal access and measurement.
- (iii) Integration of NFC functionality for individual animal identification.
- (iv) Sufficiently lightweight form factor that does not interfere with natural, freely moving behavior.

The crown configurations were fabricated to meet different experimental needs. The slide-lid design featured tapered rectangular geometry, incorporating a grid-patterned lid to reduce weight (0.79 g) (Figs. 3a, S5). The screw-cap design utilized a threaded locking mechanism for enhanced mechanical stability, with a total weight of 0.99 g (Figs. 3b, S5). Both versions were produced using 3D printing, maintained a compact height of 18–20 mm, and were sufficiently lightweight to avoid interference with natural mouse behavior (Fig. 3a, b). Beyond their lightweight profile, both crown designs feature a substantial internal volume of up to approximately 2000 mm<sup>3</sup>, providing significant scalability for future upgrades. This ample space allows for the seamless integration of miniaturized hardware—such as wireless transmission modules or inductive power circuits—without requiring further structural modifications. The closed-crown packaging robustly protects integrated components while maintaining the animal's behavioral freedom.

An NFC tag was embedded inside the crown lid, enabling efficient and accurate identification of individual animals (Movie S3). This feature streamlined the management of neural data in multi-animal experiments and minimized errors from misidentification. Moreover, it eliminated the need for conventional identification methods such as ear punching or repeated tail marking, thereby improving practical applicability. The NFC-based identification allowed recognition simply by bringing a standard smartphone close to the crown (Movie S3).

During assembly, the neural probe system was first secured to the skull, the flexible cable was connected, and the crown was closed to fully enclose the system, providing protection against mechanical impact, contamination, and bite-induced damage (Fig. 3c, d).

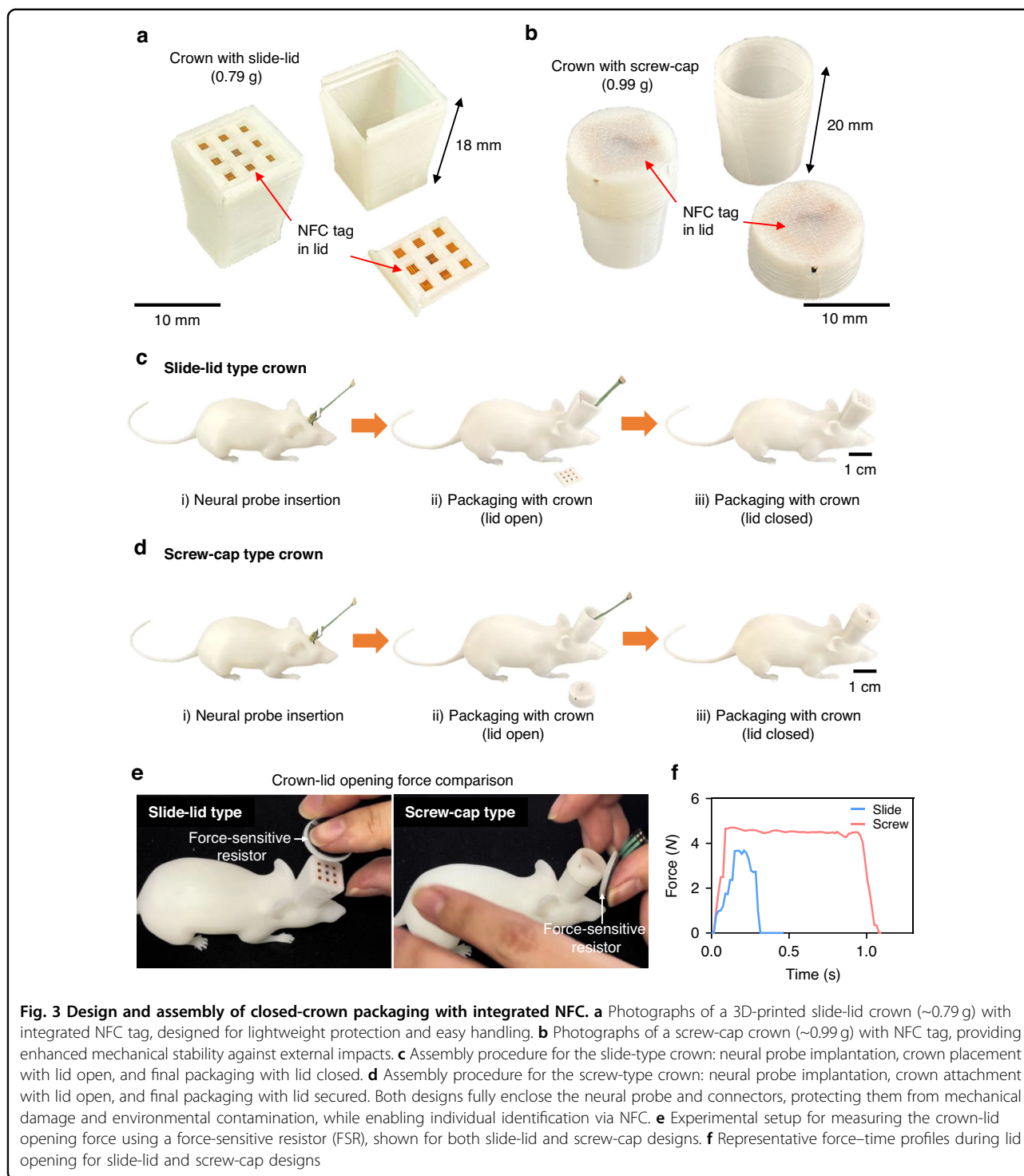
The assembled system remained lightweight (<2 g) and compact, allowing unrestricted movement during behavioral experiments and long-term group housing<sup>58</sup>. The crown maintained secure attachment over repeated sessions, ensuring stable, long-term performance. By providing structural scalability for various module upgrades, the proposed system establishes a versatile experimental platform for neural recording. Collectively, these design features enhance experimental reliability, operational efficiency, and feasibility for large-scale, multi-animal neural recording studies.

### Characterization and evaluation of the closed-crown packaging system

The closed-crown packaging system was further evaluated to assess its mechanical robustness, practical usability, and behavioral compatibility under group-housing conditions. This evaluation focused on three aspects: (i) the lid-opening mechanics of the two crown designs, (ii) a direct comparison with conventional protection strategies, and (iii) the behavioral effects of crown mounting.

First, the force and duration required for lid opening were quantitatively measured for the slide-lid and screw-cap designs (Fig. 3e and Movie S4). The slide-lid type required a peak opening force of up to 3.68 N and could be opened in approximately 0.5 s (Fig. 3f). In contrast, the screw-cap type required a higher peak force of approximately 4.7 N, which had to be applied continuously for about 1.1 s to fully open the lid (Fig. 3f). The slide-lid type therefore required a lower opening force and enabled faster access, resulting in a lightweight configuration (~0.79 g) suitable for experiments involving frequent connection and disconnection of the probe interface. This design provided sufficient mechanical stability in typical group-housing environments involving small and low-aggression strains such as C57BL/6J. In contrast, the screw-cap type, owing to its threaded locking mechanism, demanded higher torque and longer opening time. Although slightly heavier (~0.99 g), it exhibited superior resistance to external forces and animal–animal interactions, making it more suitable for larger or more aggressive strains (e.g., CD-1 or BALB/c), socially competitive colonies, or cages with frequent physical contact. These results indicate that the two crown types offer complementary advantages, allowing researchers to select the appropriate configuration based on experimental goals, animal strain, and housing conditions. While this study provides initial evidence of performance under routine social interactions, the structural robustness of the screw-cap design suggests potential for maintaining integrity during high-intensity behaviors, such as aggression, physical contests, or other complex social behaviors.

Next, the protective efficacy of the closed-crown system was directly compared with conventional open-crown packaging and a medical-tape-based temporary encapsulation under identical group-housing conditions. Mice were initially implanted with the neural probe and crown assembly and allowed a one-week postoperative recovery period (Fig. S6). In the open-crown condition, exposed cables were repeatedly bitten and pulled by cage mates, resulting in partial cable damage in most animals within 7.5 h and complete cable breakage in all animals within 48 h (Fig. S7, S8 and Movie S5). The tape-based encapsulation provided only transient protection; most tapes partially detached within 24 h, and in at least one animal



in which the tape was fully detached, severe cable damage was observed by day 2 (Fig. S9). In contrast, the closed-crown system fully enclosed the cable and connector, preventing access by other animals and eliminating bite-induced mechanical damage throughout the observation period (Fig. S7).

Finally, behavioral assessments were conducted to verify that the closed-crown system itself did not interfere with locomotor activity or anxiety-related behavior. After implantation of the screw-type closed-crown system, the body weight of mice increased by an average of 1.32 g, corresponding to the combined mass of the crown, neural

probe, and dental cement (Fig. S10a). Following a one-week postoperative recovery period, each experimental group was group-housed separately under identical housing conditions. Body weight trajectories showed consistent increases in both groups, with approximately a 10% increase observed by week 3, indicating normal growth and recovery irrespective of crown mounting (Fig. S10b). Open field tests revealed no significant differences between crown-mounted and control mice in total distance traveled, center-zone exploration, or overall movement patterns across multiple weeks (Fig. S11, S12). These findings indicate that the closed-crown system, owing to its lightweight design, does not measurably affect locomotion or anxiety-related behavior.

Overall, this evaluation demonstrates that the closed-crown packaging system offers a robust, flexible, and behaviorally neutral solution for chronic neural recording in group-housed animals, overcoming key limitations of conventional encapsulation strategies. Future research will evaluate the system's performance under high-intensity behaviors.

#### Long-term neural recording stability in group-housed mice

We next evaluated whether the closed-crown packaging system enables long-term, stable neural recording under group-housing conditions. Silicon neural probes were implanted into the hippocampal CA1 region of adult mice, followed by a one-week recovery period (Fig. S13). The animals were then returned to group-housed cages, and impedance and neural spike activity were monitored over an extended recording period (Fig. 4a).

A total of six mice were tested in group-housed condition. Impedance and spike signals were recorded on day 0 (post-implantation) and subsequently at weekly intervals. Recordings were conducted in awake animals, which were briefly transferred to an isolated chamber for signal acquisition.

Impedance variation, a key indicator of system stability, was analyzed to assess the long-term reliability of the implanted electrodes. Although impedance initially increased shortly after implantation—likely due to glial encapsulation and the foreign body response<sup>36,46,59</sup>—it remained stable from week 1 onward without significant fluctuations (Fig. 4b). This result demonstrates that the closed-crown system can maintain stable recordings over extended periods, even under socially enriched housing conditions, whereas conventional open-crown systems often fail due to cable damage or disconnection (Figs. S1, S8).

Neural signal quality was maintained over extended recording periods in group-housed mice using the closed-crown system for 3 weeks (Fig. 4c, d). In additional experiments, mice implanted with the same closed-crown configuration were recorded for up to 5 weeks after group

housing (Fig. S14). Across eight recording channels, stable spike activity was repeatedly detected in four channels, while the remaining channels consistently exhibited comparable noise levels.

Analysis of spike waveforms confirmed preserved morphology over time, whereas the signal-to-noise ratio (SNR) showed a gradual decline at later time points. Specifically, higher SNR values were observed during the initial 1–2 weeks, followed by a progressive reduction by weeks 4–5 (Fig. S15). This trend is consistent with well-documented *in vivo* tissue responses—such as microglial activation and astrocytic encapsulation—that increase the electrode–neuron distance during chronic implantation<sup>32,36</sup>, rather than reflecting a structural or mechanical failure of the closed-crown system itself.

Collectively, these results validate that the closed-crown system supports long-term neural recordings in group-housed mice. By providing mechanical stability and physical protection for the probe and cables, this approach establishes a powerful experimental platform for chronic monitoring of neural circuit dynamics in relation to social behavior over extended periods.

#### Preservation of social interaction behavior under chronic recording conditions

To investigate how housing conditions affect social behavior, we conducted a social interaction test comparing group-housed and isolated-housed mice implanted with the closed-crown system. The behavioral arena consisted of an opaque acrylic chamber (35 × 25 × 25 cm<sup>3</sup>), with a transparent acrylic cage featuring 5 mm vertical bars attached to one side to hold an unfamiliar conspecific (Figs. 5a, S16). This arrangement allowed the test mouse to approach the stimulus animal from three sides. A 7.5 cm zone surrounding the cage, referred to as the gray-shaded zone, was defined to quantitatively assess social interaction (Fig. 5b).

Behavioral experiments were conducted weekly for six weeks under both housing conditions (Movie S6). During each 10-minute session, mice freely explored the arena, and their trajectories and behaviors were tracked using IDTracker software (Fig. 5c). The following metrics were quantified: total distance traveled, distance traveled within the gray-shaded zone, time spent in the gray-shaded zone, and total social interaction time with the unfamiliar mouse.

Results indicated no significant differences in overall locomotor activity or gray-shaded zone exploration between the two groups (Fig. 5d). However, social interaction time revealed distinct patterns over repeated sessions. Group-housed mice displayed high initial interaction, likely due to novelty-driven curiosity, which declined sharply in subsequent sessions (Fig. 5d). Isolated-housed mice exhibited a sharp decrease in social

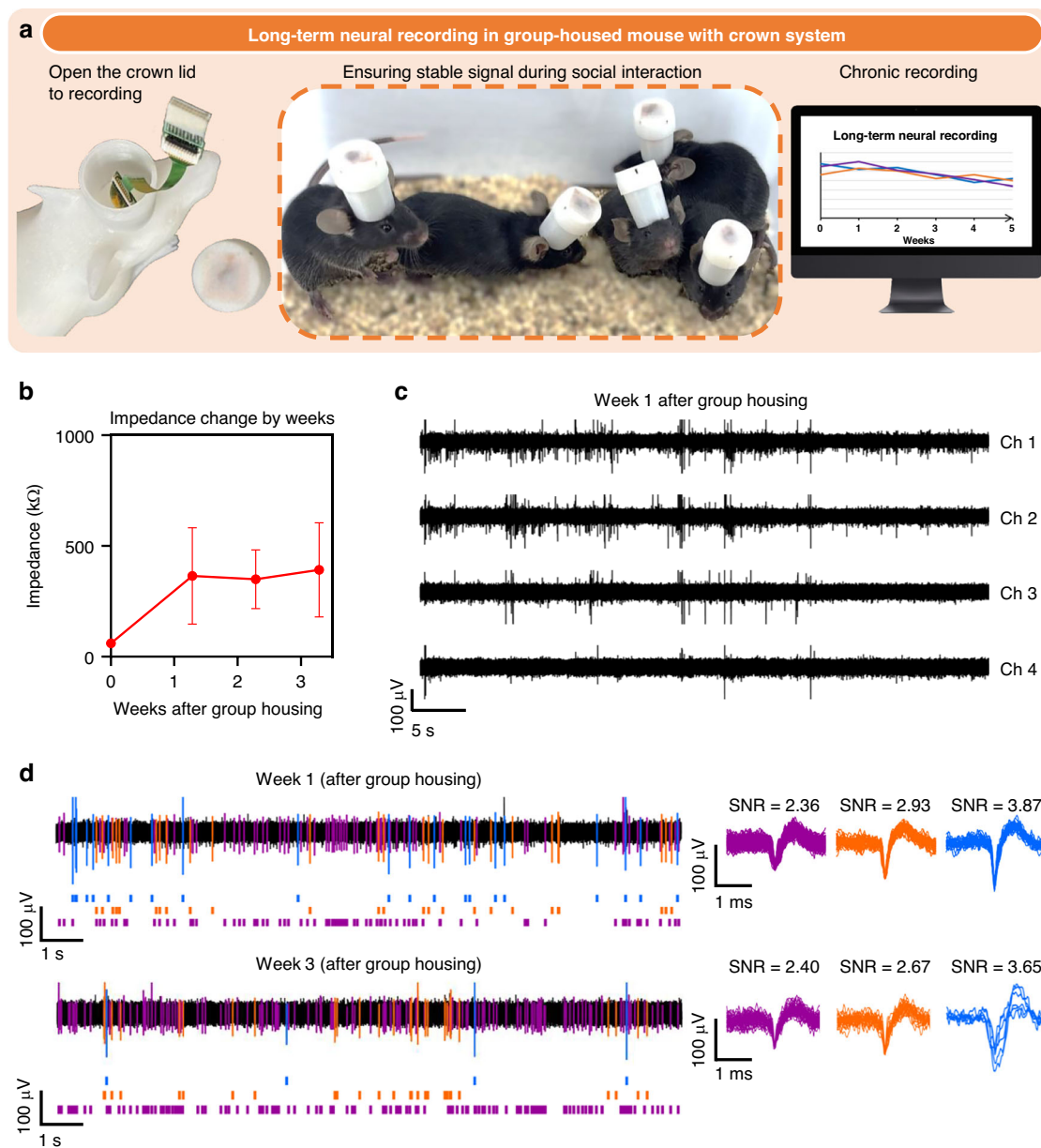


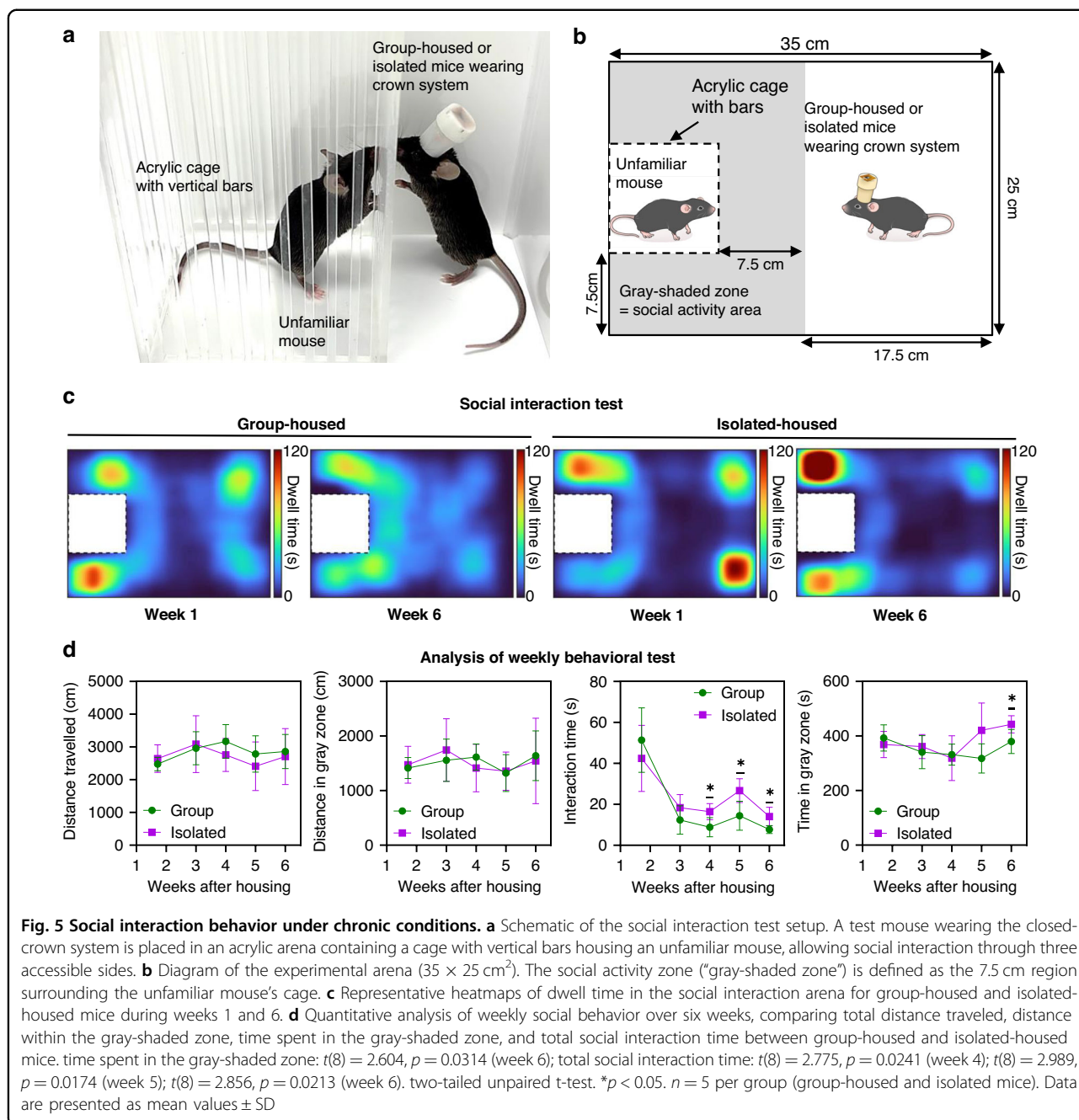
**Fig. 4** Long-term neural recording stability in group-housed mice using the closed-crown system. **a** Schematic and experimental setup for chronic neural recording in group-housed mice, showing that the crown lid can be opened for electrophysiological access. **b** Longitudinal changes in electrode impedance measured weekly after probe implantation and initiation of group housing.  $n = 6$  (Mice). **c** Representative neural spike traces recorded from four channels (Ch 1–4) one week after group housing. **d** Representative raster plots and corresponding spike waveforms recorded at 1 and 3 weeks after group housing, demonstrating consistent firing activity and preserving spike shapes over time. Data are presented as mean values  $\pm$  SD

interaction time after the first session, followed by a partial rebound and sustained higher interaction levels compared with group-housed mice, resulting in a statistically significant difference between groups over time (Fig. 5d).

A similar trend was observed in the time spent within the gray-shaded zone. Group-housed mice maintained relatively stable proximity to the unfamiliar mouse,

whereas isolated-housed mice exhibited a progressive increase in time spent near the stimulus animal starting at week 5, reaching a marked difference by week 6 (Fig. 5d).

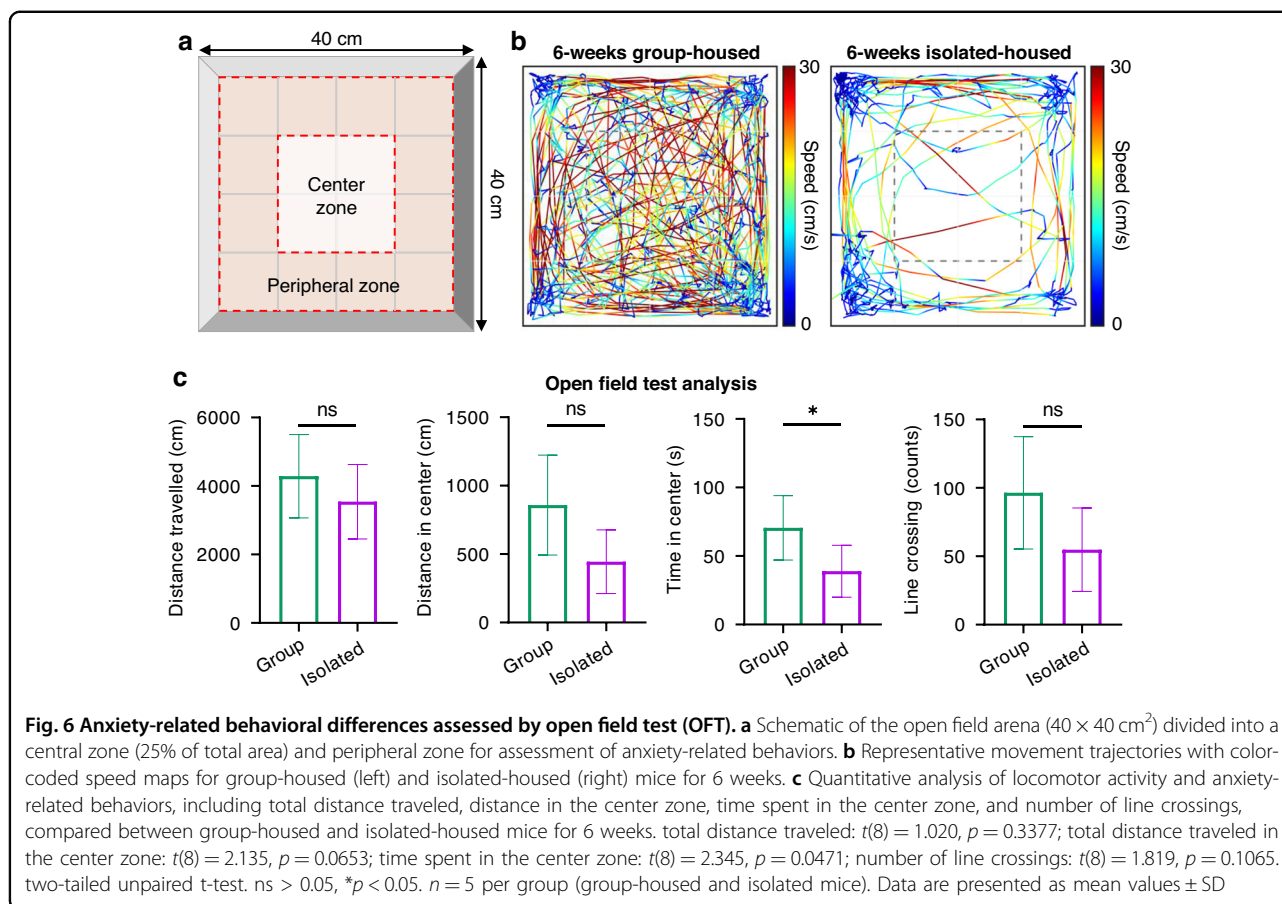
To further dissociate the effects of housing conditions from any potential influence of the packaging system itself, we additionally performed the same social interaction test in normal (non-implanted) mice under identical experimental protocols (Movie S7). Group-housed and



isolated-housed normal mice were tested weekly for four weeks using the same arena configuration, analysis pipeline, and behavioral metrics as those applied to the closed-crown–implanted groups. Consistent with the results observed in closed-crown–implanted animals, group-housed normal mice exhibited a progressive reduction in social interaction time with the unfamiliar conspecific across repeated sessions, whereas isolated-housed normal mice maintained relatively elevated interaction levels over time (Fig. S17, S18). A similar divergence was observed in the time spent within the gray-shaded

interaction zone, with isolated-housed mice showing increased dwell time compared with group-housed mice at later weeks (Fig. S18b).

These findings demonstrate that the closed-crown packaging system preserves natural social interaction in group-housing conditions. By maintaining normal behavioral patterns without inducing stress or artifacts, this system provides a powerful platform for investigating the neural basis of social interaction and its modulation by environmental context, offering a significant advantage over conventional approaches.



### Anxiety-related behavioral differences revealed by open field test

To further investigate the effects of housing conditions on anxiety-related behavior<sup>51,52</sup>, we conducted an open field test (OFT) in closed-crown-implanted mice that were group-housed or isolated for six weeks. The behavioral arena was constructed from opaque acrylic ( $40 \times 40 \text{ cm}^2$ ) and divided using a virtual grid into a central zone (center 25%) and a peripheral zone (Fig. 6a). Each mouse was allowed to freely explore the arena for 10 minutes, and locomotor trajectories and behaviors were analyzed using IDTracker software (Fig. 6b and Movies S8, S9). Metrics quantified included total distance traveled, distance traveled within the center zone, time spent in the center zone, and number of line crossings. The same animals used in the social interaction experiments—housed either in group or isolation conditions for six weeks—were tested.

Behavioral analysis revealed that isolated-housed mice exhibited reduced locomotor activity, decreased center zone exploration, shorter time spent in the center, and fewer line crossings compared with group-housed mice (Fig. 6c). Notably, time spent in the center zone differed significantly between groups: isolated mice spent

considerably less time in the central area and preferentially remained near the corners, behaviors typically associated with elevated anxiety.

Importantly, similar behavioral trends were observed in normal (non-implanted) mice subjected to the same housing conditions. Isolated normal mice displayed a progressive reduction in center-zone distance and dwell time over weeks, whereas these measures remained relatively stable in group-housed normal mice (Fig. S19). These patterns are consistent with classical anxiety-like phenotypes induced by prolonged social isolation. Correspondingly, body weight analysis revealed that isolated normal mice exhibited a transient but significant weight loss (~2%) at week 3 compared with week 2, whereas group-housed normal mice maintained stable body weight over time (Fig. S20). This physiological change further supports the presence of chronic stress in isolated animals.

Together, these results demonstrate that social isolation increases anxiety-related behaviors regardless of crown implantation, while group housing preserves normal exploratory and locomotor patterns. This finding confirms that the closed-crown system itself does not induce behavioral artifacts and underscores the

importance of maintaining group-housing conditions for reliable behavioral assessment and chronic neural recording experiments.

## Conclusions

In this study, we developed and experimentally validated a closed-crown packaging system that enables long-term and stable neural recordings in group-housed mice. The system overcomes key limitations of conventional open-crown designs—such as frequent cable breakage, component damage, and device failure—thereby ensuring the continuity of chronic experiments in group-housing conditions.

The system's performance is achieved through three major innovations. First, NFC-enabled closed-crown packaging protects the probe and connectors from mechanical impact, biting, and contamination while facilitating individual identification and efficient data management. Second, the lightweight overall design minimizes behavioral stress and preserves normal social interactions in group-housing conditions. Third, an ultrathin flexible cable fabricated using PSR reduces cable thickness to roughly one-third of conventional designs, enhancing mechanical flexibility, stability, and reliable signal transmission even under repeated movement or connection cycles.

Using this platform, we demonstrated stable impedance profiles and sustained spike detectability over multiple weeks in group-housed mice. Although signal-to-noise ratio (SNR) showed a gradual decline over extended recording periods—consistent with well-known tissue responses in chronic silicon probe implants—spike waveform morphology and recording continuity were maintained, indicating that the observed signal changes were not attributable to mechanical instability or packaging failure. Importantly, behavioral assays confirmed that the closed-crown system itself does not disrupt natural locomotor activity or induce anxiety-related behavioral artifacts.

Social interaction and open field tests further revealed that behavioral alterations associated with social isolation, such as increased anxiety-related behavior and prolonged social interaction, were consistently observed regardless of crown implantation. In contrast, group-housed mice—both with and without the closed-crown system—maintained normal exploratory and social behavior. These findings demonstrate that the closed-crown packaging preserves natural behavior while enabling chronic neural recording under socially relevant housing conditions.

From a practical neuroscience perspective, this study shifts the focus from device-level reliability to system-level stability under realistic behavioral and social conditions. Rather than optimizing individual components in isolation, our work highlights the importance of integrated

packaging strategies that ensure long-term functionality in group-housed environments.

Future directions include (i) extending recording periods using material strategies such as lubricant coatings<sup>36</sup> or immunosuppressive treatments<sup>32</sup>; (ii) integrating wireless modules with wireless power transfer capability<sup>60,61</sup>, facilitated by the reserved internal space within the current crown design, to eliminate potential behavioral constraints associated with tethered cable connections; (iii) adapting the closed-crown platform for compatibility with high-density neural electrode architectures<sup>27,28,62</sup>; and (iv) evaluating the mechanical integrity of the screw-cap crown during high-intensity social behaviors to further expand the system's application range. Although behavioral experiments in this study were conducted without tethered cable connections, these advances will allow long-term, large-scale acquisition of neural and behavioral data under more naturalistic conditions by fully removing tether-related behavioral influences.

In summary, the closed-crown packaging system establishes a practical and scalable framework for chronic neural recording in group-housed animals while preserving natural social behavior. This platform provides a powerful tool for investigating how social stimuli shape neural circuits and behavior and holds promise for advancing our understanding and treatment of social-behavior-related neuropsychiatric disorders, including depression and anxiety.

## Acknowledgements

This research was supported by the Bio & Medical Technology Development Program of the National Research Foundation (NRF) funded by the Korean government (MSIT) (RS-2025-02243041). This work was supported by the National Research Foundation of Korea (NRF) grant funded by the Korean government (MSIT) (RS-2025-00557203, RS-2021-NR062074). This research was supported by the Basic Science Research Program through the National Research Foundation of Korea (NRF), funded by the Ministry of Education (RS-2025-25423539). This work has also been supported by the Korea Brain Research Institute research program funded by the Ministry of Science and ICT (25-BR-02-02, 25-BR-04-01).

## Author details

<sup>1</sup>School of Electronics Engineering, Kyungpook National University, Daegu, Republic of Korea. <sup>2</sup>School of Electronic and Electrical Engineering, Kyungpook National University, Daegu, Republic of Korea. <sup>3</sup>Emotion, Cognition & Behavior Research Group, Korea Brain Research Institute (KBRI), Daegu, Republic of Korea. <sup>4</sup>Graduate School, Daegu Gyeongbuk Institute of Science and Technology (DGIST), Daegu, Republic of Korea. <sup>5</sup>Brain Science and Engineering Institute, Kyungpook National University, Daegu, Republic of Korea

## Author contributions

Y.H. designed and performed the majority of the experiments. G.K., H.L., H.C., M.K. and S.H.P. contributed to measurement experiments and data acquisition. S.L. contributed to the *in vivo* experiments. N.C. and H.S. supervised the project and provided critical revisions to the manuscript. Y.H. and H.S. wrote the manuscript with input from all authors. All authors discussed the results and approved the final manuscript.

**Ethics approval and consent to participate**

All animal experiments were approved by the Institutional Animal Care and Use Committee (IACUC) of the Korean Brain Research Institute (KBRI) (Approval No. IACUC-25-00039-M1) and were conducted in accordance with relevant guidelines and regulations.

**Conflict of interest**

The authors declare no competing interests.

**Supplementary information** The online version contains supplementary material available at <https://doi.org/10.1038/s41378-026-01293-2>.

Received: 13 November 2025 Revised: 18 February 2026 Accepted: 20 March 2026

Published online: 11 May 2026

**References**

- Yue, F. et al. A comparative encyclopedia of DNA elements in the mouse genome. *Nature* **515**, 355–364 (2014).
- Breschi, A., Gingeras, T. R. & Guigo, R. Comparative transcriptomics in human and mouse. *Nat Rev Genet* **18**, 425–440 (2017).
- Wong, H. H., Chou, C. Y. C., Watt, A. J. & Sjöström, P. J. Comparing mouse and human brains. *Elife* **12** <https://doi.org/10.7554/eLife.90017> (2023).
- Ellenbroek, B. & Youn, J. Rodent models in neuroscience research: is it a rat race?. *Dis Model Mech* **9**, 1079–1087 (2016).
- Yang, M., Silverman, J. L. & Crawley, J. N. Automated three-chambered social approach task for mice. *Curr Protoc Neurosci* **8**, 26 (2011).
- Zheng, H. et al. Behavioral tests for the assessment of social hierarchy in mice. *Front Behav Neurosci* **19**, 1549666 (2025).
- Choe, I. H. et al. Mice in social conflict show rule-observance behavior enhancing long-term benefit. *Nat Commun* **8**, 1176 (2017).
- Wang, F. et al. Bidirectional control of social hierarchy by synaptic efficacy in medial prefrontal cortex. *Science* **334**, 693–697 (2011).
- Sullivan, C. R. P., Olsen, S. & Widge, A. S. Deep brain stimulation for psychiatric disorders: From focal brain targets to cognitive networks. *Neuroimage* **225**, 117515 (2021).
- Soleimani, G. et al. Closing the loop between brain and electrical stimulation: towards precision neuromodulation treatments. *Transl Psychiatry* **13**, 279 (2023).
- Yang, D., Shin, Y. I. & Hong, K. S. Systemic Review on Transcranial Electrical Stimulation Parameters and EEG/fNIRS Features for Brain Diseases. *Front Neurosci* **15**, 629323 (2021).
- Rao, V. R. et al. Direct Electrical Stimulation of Lateral Orbitofrontal Cortex Acutely Improves Mood in Individuals with Symptoms of Depression. *Curr Biol* **28**, 3893–3902 e3894 (2018).
- Li, H., Wang, J. & Fang, Y. Recent developments in multifunctional neural probes for simultaneous neural recording and modulation. *Microsyst Nanoeng* **9**, 4 (2023).
- Malekshoaraie, M. H. et al. Fully flexible implantable neural probes for electrophysiology recording and controlled neurochemical modulation. *Microsyst Nanoeng* **10**, 91 (2024).
- Park, S. et al. A depth-customizable double-sided 3D neural probe array for simultaneous investigation of multiple brain regions. *Sensors Actuators A: Phys* **395** <https://doi.org/10.1016/j.sna.2025.117084> (2025).
- Kim, M. et al. Depth-customizable 3D electrode array for recording functional connectivity in the brain. *Adv Electron Mater* **11** <https://doi.org/10.1002/aeml.202500121> (2025).
- Boyden, E. S., Zhang, F., Bamberg, E., Nagel, G. & Deisseroth, K. Millisecond-timescale, genetically targeted optical control of neural activity. *Nat Neurosci* **8**, 1263–1268 (2005).
- Deisseroth, K. Optogenetics. *Nat Methods* **8**, 26–29 (2011).
- Shin, H. et al. Transcranial optogenetic brain modulator for precise bimodal neuromodulation in multiple brain regions. *Nat Commun* **15**, 10423 (2024).
- Zhang, Y. et al. Fast and sensitive GCaMP calcium indicators for imaging neural populations. *Nature* **615**, 884–891 (2023).
- Chen, T. W. et al. Ultrasensitive fluorescent proteins for imaging neuronal activity. *Nature* **499**, 295–300 (2013).
- Chou, N. et al. A multimodal multi-shank fluorescence neural probe for cell-type-specific electrophysiology in multiple regions across a neural circuit. *Adv Sci* **9**, e2103564 (2022).
- Shin, H. et al. Interference-free, lightweight wireless neural probe system for investigating brain activity during natural competition. *Biosens Bioelectron* **195**, 113665 (2022).
- Yoon, Y. et al. Neural probe system for behavioral neuropharmacology by bi-directional wireless drug delivery and electrophysiology in socially interacting mice. *Nat Commun* **13**, 5521 (2022).
- Yang, Y. et al. Wireless multilateral devices for optogenetic studies of individual and social behaviors. *Nat Neurosci* **24**, 1035–1045 (2021).
- Guo, C. et al. Miniscope-LFOV: A large-field-of-view, single-cell-resolution, miniature microscope for wired and wire-free imaging of neural dynamics in freely behaving animals. *Sci Adv* **9**, eadg3918 (2023).
- Steinmetz, N. A. et al. Neuropixels 2.0: A miniaturized high-density probe for stable, long-term brain recordings. *Science* **372** <https://doi.org/10.1126/science.abf4588> (2021).
- Trautmann, E. M. et al. Large-scale high-density brain-wide neural recording in nonhuman primates. *Nat Neurosci* **28**, 1562–1575 (2025).
- Dhawale, A. K. et al. Automated long-term recording and analysis of neural activity in behaving animals. *Elife* **6** <https://doi.org/10.7554/eLife.27702> (2017).
- Wang, Y., Yang, X., Zhang, X., Wang, Y. & Pei, W. Implantable intracortical microelectrodes: reviewing the present with a focus on the future. *Microsyst Nanoeng* **9**, 7 (2023).
- Schroder, T. et al. The DREAM Implant: A Lightweight, Modular, and Cost-Effective Implant System for Chronic Electrophysiology in Head-Fixed and Freely Behaving Mice. *J Vis Exp* <https://doi.org/10.3791/66867> (2024).
- Chae, U. et al. KDS2010, a reversible MAO-B inhibitor, extends the lifetime of neural probes by preventing glial scar formation. *Glia* **72**, 748–758 (2024).
- Song, Z. M. et al. Chronic, reusable, multiday neuropixels recordings during free-moving operant behavior. *Eneuro* **11** <https://doi.org/10.1523/Eneuro.0245-23.2023> (2024).
- Mueller, N. N. et al. Mechanically-adaptive, resveratrol-eluting neural probes for improved intracortical recording performance and stability. *Npj Flex Electron* **9**, 64 (2025).
- Won, C. et al. Mechanically Tissue-Like and Highly Conductive Au Nanoparticles Embedded Elastomeric Fiber Electrodes of Brain-Machine Interfaces for Chronic In Vivo Brain Neural Recording. *Adv Funct Mater* **32** <https://doi.org/10.1002/adfm.202205145> (2022).
- Lee, Y. et al. A Lubricated Nonimmunogenic Neural Probe for Acute Insertion Trauma Minimization and Long-Term Signal Recording. *Adv Sci (Weinh)* **8**, e2100231 (2021).
- Zhang, S. et al. A removable insertion shuttle for ultraflexible neural probe implantation with stable chronic brain electrophysiological recording. *Adv Mater Interfaces* **7** <https://doi.org/10.1002/admi.201901775> (2020).
- Park, S. et al. Adaptive and multifunctional hydrogel hybrid probes for long-term sensing and modulation of neural activity. *Nat Commun* **12**, 3435 (2021).
- Park, S. et al. One-step optogenetics with multifunctional flexible polymer fibers. *Nat Neurosci* **20**, 612–619 (2017).
- Fone, K. C. & Porkess, M. V. Behavioural and neurochemical effects of post-weaning social isolation in rodents-relevance to developmental neuropsychiatric disorders. *Neurosci Biobehav Rev* **32**, 1087–1102 (2008).
- Ieraci, A., Mallei, A. & Popoli, M. Social isolation stress induces anxious-depressive-like behavior and alterations of neuroplasticity-related genes in adult male mice. *Neural Plast* **2016**, 6212983 (2016).
- Han, R. T. et al. Long-term isolation elicits depression and anxiety-related behaviors by reducing oxytocin-induced GABAergic transmission in central amygdala. *Front Mol Neurosci* **11**, 246 (2018).
- Benfato, I. D. et al. Effects of long-term social isolation on central, behavioural and metabolic parameters in middle-aged mice. *Behav Brain Res* **417**, 113630 (2022).
- Villalón, S. A., Felix-Ortiz, A. C., Lozano-Ortiz, K., McCarrey, J. R. & Burgos-Robles, A. Impacts of social isolation stress in safety learning and the structure of defensive behavior during a spatial-based learning task involving thermal threat. *Front Behav Neurosci* **18**, 1503097 (2024).
- Grigoryan, G. A., Pavlova, I. V. & Zaichenko, M. I. Effects of social isolation on the development of anxiety and depression-like behavior in model experiments in animals. *Neurosci Behav Physiol* **52**, 722–738 (2022).

46. Shin, H. et al. Multifunctional multi-shank neural probe for investigating and modulating long-range neural circuits in vivo. *Nat Commun* **10**, 3777 (2019).
47. Shin, H. et al. 3D high-density microelectrode array with optical stimulation and drug delivery for investigating neural circuit dynamics. *Nat Commun* **12**, 492 (2021).
48. Lee, H. et al. A Highly Efficient Low-Cost Flexible Neural Probe for Scalable Mass Fabrication. *ACS Omega* **10**, 10733–10740 (2025).
49. Lee, H. et al. Low-cost, high-efficiency double-sided neural probe. *Sensor Actuat a-Phys* **387** <https://doi.org/10.1016/j.sna.2025.116437> (2025).
50. Paxinos, G. & Franklin, K. B. J. *The mouse brain in stereotaxic coordinates*. Compact 2nd edn, (Elsevier Academic Press, 2004).
51. Tatem, K. S. et al. Behavioral and locomotor measurements using an open field activity monitoring system for skeletal muscle diseases. *J Vis Exp*, 51785 (2014).
52. Seibenhener, M. L. & Wooten, M. C. Use of the Open Field Maze to measure locomotor and anxiety-like behavior in mice. *J Vis Exp*, e52434 <https://doi.org/10.3791/52434> (2015).
53. Ferlauto, L. et al. Development and Characterization of PEDOT:PSS/Alginate Soft Microelectrodes for Application in Neuroprosthetics. *Front Neurosci* **12**, 648 (2018).
54. Sim, S. et al. Neural probe integrated with low-impedance electrodes implemented using vertically aligned carbon nanotubes for three-dimensional mapping of neural signals. *Sensor Actuat B-Chem* **393** <https://doi.org/10.1016/j.snb.2023.134124> (2023).
55. Trainor, B. C. et al. Sex differences in social interaction behavior following social defeat stress in the monogamous California mouse (*Peromyscus californicus*). *PLoS One* **6**, e17405 (2011).
56. Toyoda, A. Social defeat models in animal science: What we have learned from rodent models. *Anim Sci J* **88**, 944–952 (2017).
57. Ludwig, K. A. et al. Poly(3,4-ethylenedioxythiophene) (PEDOT) polymer coatings facilitate smaller neural recording electrodes. *J Neural Eng* **8**, 014001 (2011).
58. Groblewski, P. A. et al. A standardized head-fixation system for performing large-scale, in vivo physiological recordings in mice. *J Neurosci Methods* **346**, 108922 (2020).
59. Marin, C. & Fernandez, E. Biocompatibility of intracortical microelectrodes: current status and future prospects. *Front Neuroeng* **3**, 8 (2010).
60. Jung, T. et al. A wireless subdural-contained brain–computer interface with 65,536 electrodes and 1,024 channels. *Nat Electron* **8**, 1272–1288 (2025).
61. Lee, B. et al. An inductively-powered wireless neural recording and stimulation system for freely-behaving animals. *IEEE Trans Biomed Circuits Syst* **13**, 413–424 (2019).
62. Jun, J. J. et al. Fully integrated silicon probes for high-density recording of neural activity. *Nature* **551**, 232–236 (2017).